International Journal of GEOMATE, Aug., 2021, Vol.21, Issue 84, pp.228-235
ISSN: 2186-2982 (P), 2186-2990 (O), Japan, DOI: https://doi.org/10.21660/2021.84.j2199
Geotechnique, Construction Materials and Environment

THE PERFORMANCE SEA SURFACE TEMPERATURE ANOMALY OVER PACIFIC OCEAN AND NIÑO 3.4 AREA BY USING INTERMEDIATE COUPLED MODEL (ICM)

Usa Humphries[1] and *Pramet Kaewmesri[2]

[1]Department of Mathematics, Faculty of Science, King Mongkut's University of Technology Thonburi (KMUTT), Bangkok, Thailand
[2]Geo-Informatics and Space Technology Development Agency, Bangkok, Thailand

*Corresponding Author, Received: 11 May 2021, Revised: 01 June 2021, Accepted: 13 June 2021

ABSTRACT: In this research, climate variability is discussed as the main important problem in the world. Because the extreme event has impacted the naturally changed and the results of the naturally changed are many severe damages varying accordingly in a wide range of territory over the world. These damages include storms, sea-level rise, floods, and droughts. The El Niño-Southern Oscillation (ENSO) is one of the primaries of the climate variability under current concern. Therefore, the aim of this research is to study the mechanism of Sea Surface Temperature Anomaly (SSTA) during 2011–2020 and simulate SSTA over the Pacific Ocean and Niño 3.4 area in advance. The results of ICM are compared with the Extended Reconstructed Sea Surface Temperature (ERSST) observation dataset. Through time series analysis, the result from the ICM model can capture the highest value in 2016, similar to the ERSST observation. However, in the time series pattern, the results from Case I (simulation six months in advance) exhibited a good trend than Case II (simulation 12 months in advance). In statistical analysis, the values from statistical analysis, the statistical values (R, RMSE, ME, and MAE) of six months in advance revealed a good accuracy value from 12 months in advance. In conclusion, the ICM model showed high-performance results indicating simulation of SSTA over the Pacific Ocean and Niño 3.4 area, especially in the case of six months in advance.

Keywords: El Nino – Southern Oscillation, ICM model, SSTA, Pacific Ocean, Nino 3.4

1. INTRODUCTION

Climate variability has been becoming one of the main global problems at present. Because, naturally and gradually changed, a great period time to be noticeable. The variability has stayed for vary many years. Climate variability has a wide variety of dramatic impacts that cause severe damages, which vary according to a wide range of territory across the world—for example, extreme events, storms, sea-level rise, floods, and drought. One of the primary drivers of the climate variability under current concern is El Niño-Southern Oscillation (ENSO) phenomenon.

The mechanism of the ENSO phenomenon separates into three phases:

The first phase is the El Niño event. This event occurs when abnormally warm waters accumulate in tropical latitudes of the central and eastern Pacific Ocean associated with weakening the low-level easterly winds. Consequently, tropical rain usually falls over South East Asia and Australia.

The second phase is the La Nina event. This event occurs when cooler than average waters accumulate in the central and eastern tropical Pacific Ocean, associated with a strengthening of the low-level easterly winds over the central tropical Pacific Ocean. Heavy rainfall occurs over South East Asia and Australia.

The third phase is ENSO-neutral. This event is a normal event in the Pacific Ocean; strong trade wind blows from the east along the equator and pushes warm water in the western Pacific Ocean. Normal rainfall occurs over Southeast Asia and some parts of Australia.

The ENSO impact is in the areas closest to the equatorial Pacific Ocean. El Niño and La Nina are such powerful forces that can shift seasonal precipitation and temperature patterns around the globe. These movements, known as teleconnections, occur via the impact of tropical SST on the upper atmosphere.

The ENSO index calculated the average Sea Surface Temperature Anomaly (SSTA) in the Niño 3.4 area. Scientists refer to that swath as the Niño 3.4 region. The observed difference from the average temperature in that region, whether warmer or cooler, is used to indicate the current phase of ENSO.

So, one of the most challenging problems of simulation SSTA over the Pacific Ocean in the Niño 3.4. As the SSTA simulation is crucial for risk assessment in Thailand's increasingly demanding agricultural, industrial and domestic sectors [1–3], this research aims to investigate the mechanism trend SSTA during 2011–2020 and simulation

SSTA over the Pacific Ocean in the Niño 3.4 area. The results from ICM are compared with the ERSST observation dataset.

The rest of this paper is structured as follows: Section 1: Introduction of this research. Section 2: Description of the observation data, model, study area, statistical analysis method, and experiment design. Section 3: Study of ERSST observation, results from the model, and discuss results with observation data depending on time simulation. Section 4: Conclusions.

2. MATERIALS AND METHODS

This part describes methods of this research that include detail of observation data in subsection 2.1, information of the Pacific model of this research in subsection 2.2, the domain of study area in subsection 2.3, and statistical analysis in subsection 2.4.

2.1 Extended Reconstructed Sea Surface Temperature (ERSST) dataset

The Extended Reconstructed Sea Surface Temperature (ERSST) dataset is a global monthly SSTA dataset developed from the International Completeness Ocean-Atmosphere Dataset (ICOADS). The SSTA data of ERSST computed based on a 1971–2000 monthly climatology. The data production of the ERSST is on a 2°×2° global grid with statistical analysis forced spatial pattern. The spatial of ERSST cover area between latitude 0 E to 358.0 E and longitude 88 N to 88 S. The monthly period time of ERSST begins in January 1854, continuing to the present. The updated version of ERSST, version 5, utilizes new data collections from ICOADS Release 3.0. SST comes from Argo floats above 5 meters and ice concentration from Hadley Centre Ice-SST version 2. The spatial and temporal variability improves in ERSSTv5 through (a) decreasing spatial filtering in training the reconstruction functions Empirical Orthogonal Teleconnections (EOTs), (b) eliminating high latitude damping in EOTs, and (c) adding 10 more EOTs in the Arctic. ERSSTv5 improved total SST by changing from utilizing Nighttime Marine Air Temperature (NMAT) as a reference to buoy-SST as a reference in correcting ship SST biases [4–6].

In this research, the ERSST observation dataset uses to verify the results from the model. The location of the study area covers the Pacific Ocean and Niño 3.4, as shown in subsection 2.4.

2.2 Intermediate Coupled Model (ICM)

The dynamical component of ICM was developed [7], consisting of linear and non-linear components. The linear component is substantially from McCreary–type modal model [8]. A horizontally varying background stratification: ten baroclinic modes with a parameterization of local Ekman-driven upwelling are included. A correction scheme derived from the residual non-linear momentum equation that included to decrease the amplitude of zonal currents in the equatorial belt foe, which is overestimated by the linear dynamical model. As a direct result of these extensions, the model can realistically simulate the mean upper-ocean equatorial circulation and its variability [9–10].

The governing equation determining the evolution of interannual SST variability in the surface mixed layer can be written as [7]:

$$\frac{\partial \acute{T}}{\partial \bar{T}} = -\acute{u}\frac{\partial \bar{T}}{\partial x} - (\bar{U}+\acute{u})\frac{\partial \acute{T}}{\partial x} - \acute{v}\frac{\partial \bar{T}}{\partial y} - (\bar{V}+\acute{v})\frac{\partial \acute{T}}{\partial y} - [(\bar{W}+\acute{w})M(-\bar{W}-\acute{w}) - \bar{W}M(\bar{W})]\times \frac{\bar{T}_e-\bar{T}}{H} - (\bar{W}+\acute{w})M(-\bar{W}-\acute{w})\frac{\acute{T}_e-\acute{T}}{H} - \alpha\acute{T} + \frac{\kappa_h}{H}\nabla_h\left(H\nabla_h\acute{T}\right) + \frac{2\kappa_v}{H(H+H_2)}\times \left(\acute{T}_e-\acute{T}\right).$$

Here, $\acute{T}$ and $\acute{T}_e$ are anomalies of SST and the temperature of subsurface water entrained into the mixed layer; $\acute{u}$, $\acute{v}$ and $\acute{w}$ are anomalies of ocean currents (horizontal and vertical) in the surface mixed layer. H_2 is a constant (125 m); $M(x)$ is the Heaviside function; κ_h and κ_v are horizontal diffusion and vertical mixing parameters, respectively; and other variables are mean climatology fields. These components are used to calculate SST changes from the equation given above.

The domain of the ICM model covers from 33.5 S to 33.5 N and from 124 E to 70 W and includes the tropical Pacific with a realistic representation of continents. In the spatial pattern, the ICM model has a 2° zonal grid spacing and a meridional grid stretching from 0.5° within 10° of the equator to 3° at the northern and southern boundaries. Vertically, a 5500 m flat-bottom ocean is assumed; the linear component has 33 levels, chosen as in the Levitus [11], with eight levels in the upper 125 m. The two layers used to simulate the non-linear effects and high order baroclinic modes span the upper 125 m and are separated by the observed surface mixed layer [9–10].

2.3 Statistical analysis methods

The four statistical analysis methods were calculated using the Correlation Coefficient (R),

Root Mean Square Error (*RMSE*), Mean Error (*ME*), and Mean Absolute Error (*MAE*).

The value of the Correlation Coefficient (*R*) is such that $-1 \leq R \leq +1$. The positive (+) and negative (−) signs are used for positive linear correlations and negative correlations, respectively. In a positive correlation case: if the two variables have a strong positive linear correlation, *R* is close to +1. An *R*-value of exactly +1 indicates a perfect positive fit. The positive values mean a relationship between two variables in the same direction. On the other hand, negative correlation case: if the two variables have a strong negative linear correlation, *R* is close to –1. An *R*-value of exactly –1 indicates a perfect positive fit. The negative values mean a relationship between two variables in the opposite direction. The Correlation Coefficient (*R*) can be defined by the following equation:

$$R = \frac{\sum(x_i - \bar{x})(o_i - \bar{o})}{\sqrt{\sum(x_i - \bar{x})^2}\sqrt{\sum(o_i - \bar{o})^2}}$$

The value of *RMSE* close to zero indicates good simulation results, while *RMSE* is zero that means indicates a perfect model. The can be defined by the following equation:

$$RMSE = \sqrt{\frac{\sum(x_i - o_i)^2}{n}}$$

The value of *ME* measure sums the values of these errors and divides it by the number of simulations to give an average error. *ME* value near zero indicate a good estimate. If the *ME* value is zero, that means indicate a perfect estimate. The *ME* can be defined by the following equation:

$$ME = \frac{\sum(x_i - o_i)}{n}$$

The value of *MAE* measure sums the absolute values of these errors and divides it by the number of simulations to give an average error. *MAE* value near zero indicates a good estimate. If the *MAE* value is zero, that means indicate a perfect estimate. The *MAE* can be written as:

$$MAE = \frac{\sum|x_i - o_i|}{n}$$

Here, x_i is defined as the simulation variable, $\bar{x}$ is defined as the mean variable of simulation, o_i is defined as the observation variable, $\bar{o}$ is defined as the mean variable of observation, n is defined as the number of pair of observations and simulation variable, i pair of observations and simulation values. This research was focused on the *R*, *RMSE*, *ME*, and *MAE* to validate performance simulation accuracy with the observation dataset.

2.4 Domain description and experiment design

The domain experiment covers the Pacific Ocean and the Niño 3.4 area. The domain of the Pacific Ocean is situated between latitudes 33.5 S to 33.5 N and longitudes 124 E to 70 W. On the other hand, the domain of the Niño 3.4 area is situated between latitudes 5 S to 5 N and longitudes 190 E to 120 W, as shown in Fig 1.

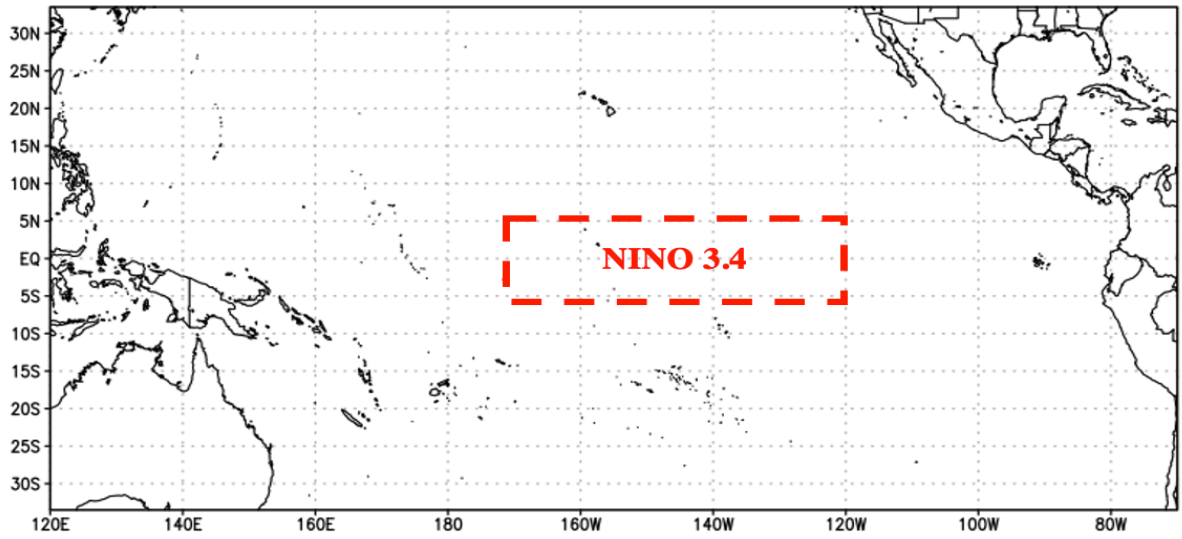

Fig 1 The domain of the Pacific Ocean and Nino 3.4 in this research

In this research, the experiment design was included three cases of SSTA simulation analysis from the ICM model. The first case analysis was from 2011 to 2015 (5 years), the second was from

2016 to 2020 (five years), and the last case analysis was from 2011 to 2020 (10 years). The model process was prepared initial data in prior December simulation year then predict the SSTA results by ICM model from January to December (January to June) in simulation 12 months in advance (six months in advance). The materials and methods are summarized in Table 1.

Table 1 Summary of the experiment design in this research

Prediction system	Detail
Pacific model	Intermediate Coupled Model (ICM)
Observation dataset	Extended Reconstructed Sea Surface Temperature (ERSST) dataset
Initial conditions	ERSST dataset in prior December simulation year
Study area	- Pacific Ocean (latitudes 33.5 S to 33.5 N and longitudes 124 E to 70 W) - Nino3.4 (latitudes 5 S to 5 N and longitudes 190 E to 120 W)
Simulation period time	2011-2020 (10 years)
Statistical analysis methods	- Correlation Coefficient (*R*), - Root Mean Square Error (*RMSE*), - Mean Error (*ME*) and Mean Absolute Error (*MAE*)
Case analysis	Case I: simulation 6 months in advance Case II: simulation 12 months in advance

3. RESULTS AND DISCUSSION

For determination of SSTA over the Pacific Ocean change in 2011–2020 observation data, which were separated in 2011–2015 (5 years) periods, in 2016–2020 (5 years) periods, and 2011–2020 (10 years) periods.

Consider analysis shows that under the influence of global SSTA in the Pacific Ocean, during 2011–2020 (almost 10 years) total amount of SSTA experience the following changes: during the period, the SSTA amount varies from 2.6 ℃ to 3.6 ℃ (Fig 3(a)). In Niño 3.4 area, during 2011–2020 (almost 10 years) total amount of SSTA experience the following changes: during the period, the SSTA amount varies from −0.2 ℃ to 2.3 ℃ (Fig 3(b)).

In period I (2011–2015), the total amount of SSTA on the Pacific Ocean change from 0.3 ℃ to 1.3 ℃. The SSTA changes from 0.3 ℃ to 1.3 ℃ (in January to June) and changes from 1.2 ℃ to 1.3 ℃ (in July to December), as shown in Fig 3(a). In Niño 3.4 area, the SSTA change from −2.7 ℃ to 2.6 ℃. The SSTA changes from −2.4 ℃ to 0.8 ℃ (in January to June) and changes from 1.4 ℃ to 2.6 ℃ (in July to December), as shown in Fig 3(b).

In period II (2016–2020), the total amount of SSTA on the Pacific Ocean changes from 1.5 ℃ to 2.7 ℃. The SSTA changes from 2.3 ℃ to 2.3 ℃ (in January to June) and changes from 2.4 ℃ to 1.5 ℃ (in July to December). In Niño 3.4 area, the SSTA change from −1.4 ℃ to 2.8 ℃. The SSTA changes from 2.2 ℃ to 1.6 ℃ (in January to June) and changes from 0.2 ℃ to −0.5 ℃ (in July to December).

However, the trend of SSTA of three cases (2011–2015, 2016–2020, and 2011–2020) shows variably SSTA. In case of the Pacific Ocean (Fig 2(a)), the maximum trend can be seen in December of 2011–2015 (1.3 ℃), April of 2016–2020 (2.7 ℃), and May of 2011–2020 (3.6 ℃), while minimum trend can be seen in January of 2011–2015 (0.3 ℃), December of 2016–2020 (1.5 ℃), and January of 2011–2020 (2.6 ℃). On the other hand, in case of the Niño 3.4 (Fig 2(b)), the maximum trend can be seen in December of 2011–2015 (2.6 ℃), March of 2016–2020 (2.8 ℃), and May of 2011–2020 (2.3 ℃); however, minimum trend is shown in January of 2011–2015 (−2.7 ℃), in November of 2016–2020 (−1.4 ℃), and January of 2011–2020 (−0.2 ℃).

According to data of SSTA (2011–2020), in the mentioned period, during two periods of 5 years. The period is observed the change in SSTA amount from 2011–2015 to 2016–2020; the annual SSTA increased by 1.3 ℃ in the Pacific Ocean case. On the other hand, in Niño 3.4, the annual SSTA increased by 0.6 ℃.

Materials of observation over the annual SSTA amount in 2011–2020 are presented in Fig 4. The maximum SSTA was recorded in 2016 (0.6 ℃) and the second maximum was recorded in 2015 (0.5 ℃), while the minimum SSTA was recorded in 2011 (–0.1 ℃) and the second minimum was recorded in 2012 (−0.1 ℃) in Pacific Ocean case. On the other hand, in Niño 3.4 case, the maximum SSTA was recorded in 2015 (1.3 ℃) and the second maximum was recorded in 2016 (0.7 ℃), while the minimum SSTA was recorded in 2011 (−0.8 ℃) and the second minimum was recorded in 2020 (−0.4 ℃).

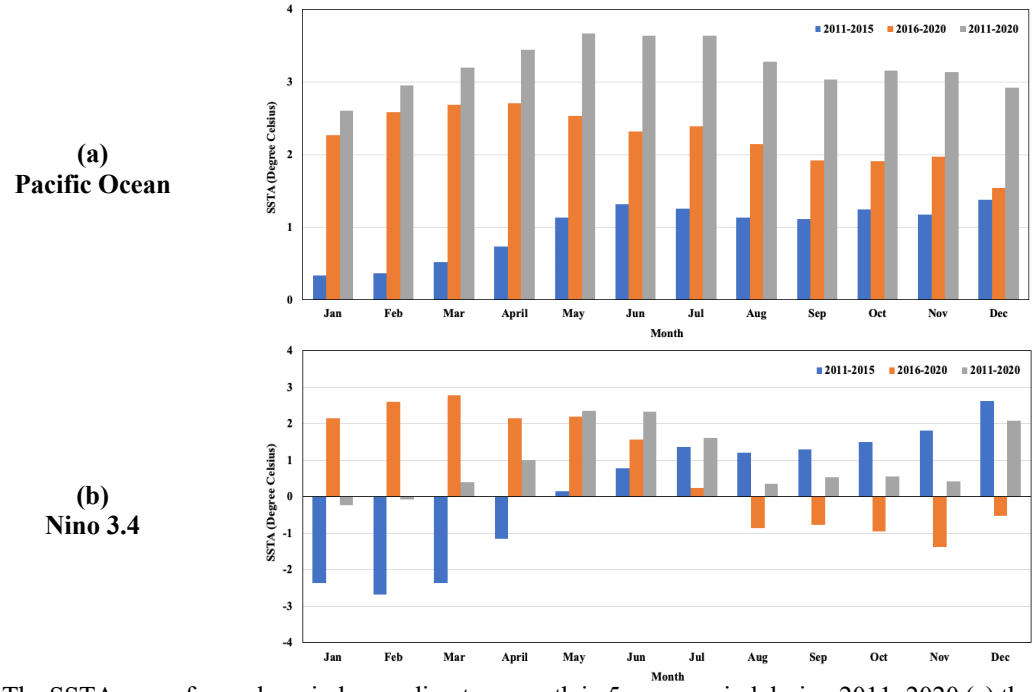

Fig 2 The SSTA mean for each period according to a month in 5 years period during 2011–2020 (a) the Pacific Ocean (b) Niño 3.4.

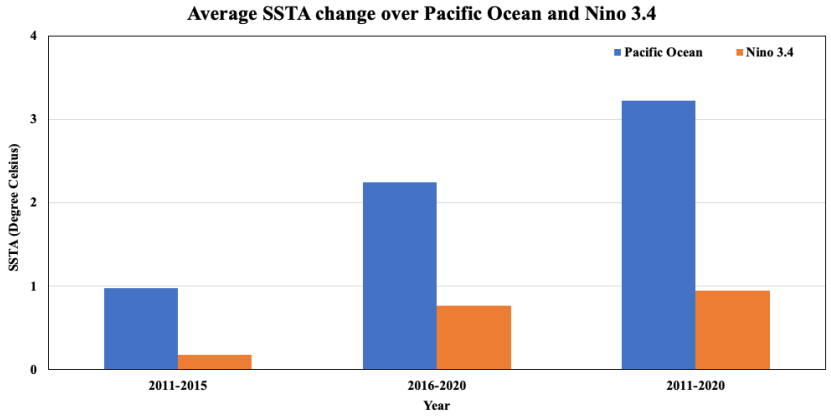

Fig 3 The SSTA mean in five years period during 2011 to 2020 over the Pacific Ocean and Niño 3.4

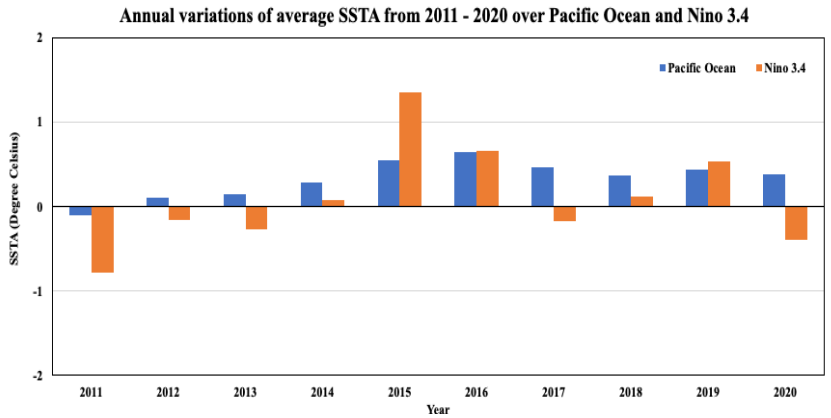

Fig 4 The annual variation of SSTA mean during 2011–2020 over the Pacific Ocean and Niño 3.4

In this research, the Pacific Ocean model (ICM model) to forecast SSTA over the Pacific Ocean and Niño 3.4 area. The prediction period was estimated from January to December from 2011 to 2020. For case analysis separate in two cases:

Case I: Simulation six months in advance (January–June)

Fig 5(a) shows the comparison of SSTA values during 2011–2020, between results from ERSST observation (blue line) and ICM model (red line) over the Pacific Ocean. The results from the ICM model showed good trend results in 2011–2016. In 2017 and 2018, the results underestimated SSTA than ERSST observation. In 2019 and 2020, the ICM model showed a good trend result than in 2017 and 2018.

Fig 5(b) shows the comparison of SSTA value during 2011–2020, between results from ERSST observation (blue line) and ICM model (red line) in over the Niño 3.4 area. The results from the ICM model showed good trend results from the 2014–2016 and 2019–2020 periods. In 2012 and 2013, the results from ICM overestimated SSTA while showing underestimate SSTA in 2017 and 2018. However, the result from the ICM model can capture the highest value in 2016, similar to ERSST observation.

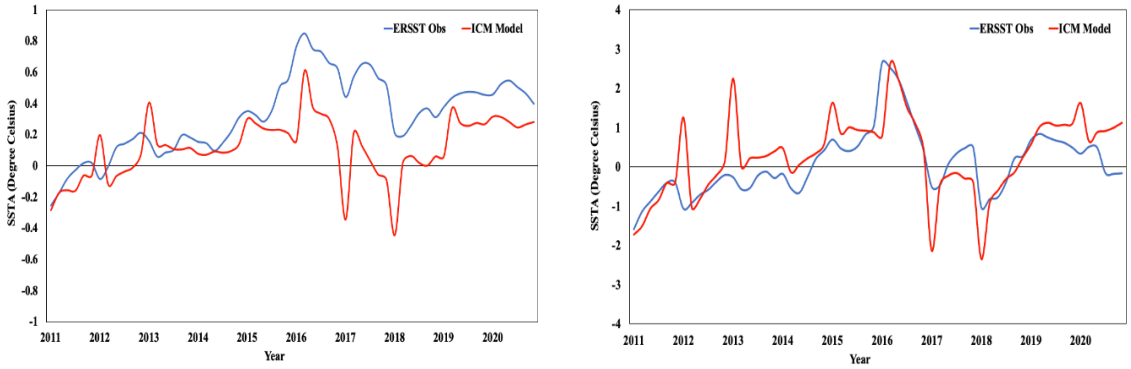

(a) (b)

Fig 5 The comparison SSTA simulation 6 months in advance (from January – June) from 2011-2020 between results from ERSST observation (blue line) and ICM model (red line) (a) Pacific Ocean (b) Nino 3.4 area.

Case II: Simulation 12 months in advance (from January – December)

In Fig 6(a), the comparison SSTA value in 2011-2020 between results from ERSST observation (blue line) and ICM model (red line) over the Pacific Ocean. The results from the ICM model were shown a good trend results in 2013-2015. Since, in 2016-2019, the results were underestimated SSTA than ERSST observation. In mid-2011 and 2013, the ICM model shown an overestimate trend result than ERSST observation.

In Fig 6(b), the comparison SSTA value in 2011-2020 between results from ERSST observation (blue line) and ICM model (red line) in over the Nino 3.4 area. The results from the ICM model were shown good trend results in the 2013-2016 and 2019-2020 periods. Since, in 2012, 2013, and 2020 the results from ICM were overestimated SSTA, while, shown underestimate SSTA in mid-2015, 2017, and 2018. However, the result from the ICM model still captures the highest value in 2016 similar to ERSST observation same Case I.

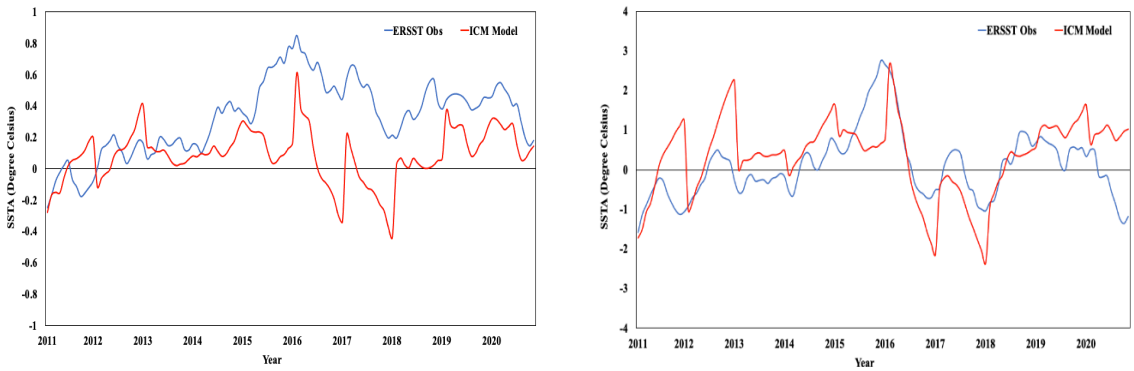

(a) (b)

Fig 6 The comparison SSTA simulation 12 months in advance (from January – June) from 2011 – 2020 between results from ERSST observation (blue line) and ICM model (red line) (a) Pacific Ocean (b) Nino 3.4 area.

The results of the ICM model can indicate a trend of SSTA time series within some period. However, in the time series pattern, the results from Case I (simulation six months in advance) showed a good trend than Case II (simulation 12 months in advance).

In this research, to quantify the ability of the ICM model to produce SSTA over the Pacific Ocean and Niño 3.4 area, the statistical value *R*, *RMSE*, *ME*, and *MAE*, as shown in Table 2.

In the Pacific Ocean, in case of the *R* values of six months in advance, good accuracy is shown in 2011–2015 (0.73), 2016–2020 (0.53), and 2011–2020 (0.56) than the value from 12 months in advance. In the case of *RMSE, ME,* and *MAE*, the value of six months in advance shows still a better value than all cases of 12 months in advance.

In Niño 3.4, the *R* values of six months in advance showed good accuracy in 2011–2015 (0.70), 2016–2020 (0.73), and 2011–2020 (0.70) than the value from 12 months in advance as same as the *R*-value from the Pacific Ocean. In the case of *RMSE, ME,* and *MAE*, the value of six months in advance show still a better value than all cases of 12 months in advance, as same as the statistical value from the Pacific Ocean.

However, in statistical analysis, the statistical value (*R, RMSE, ME* and *MAE*,) of six months in advance were given a good accuracy from the 12 months in advance, as shown in the same direction with the time series pattern in this research.

Table 2 Statistical analysis between ERSST observation and ICM model (unit: ℃).

Period time	Lead time	Statistical analysis							
		Pacific Ocean				Nino 3.4			
		R	***RMSE***	***ME***	***MAE***	***R***	***RMSE***	***ME***	***MAE***
2011–2015	06 months	**0.73**	**0.13**	**0.07**	**0.11**	**0.70**	**0.64**	**-0.40**	**0.50**
	12 months	0.35	0.23	0.11	0.18	0.42	0.90	-0.42	0.76
2016–2020	06 months	**0.53**	**0.19**	**0.34**	**0.53**	**0.73**	**0.76**	**0.01**	**0.53**
	12 months	0.41	0.20	0.39	0.54	0.60	0.91	-0.05	0.70
2011–2020	06 months	**0.56**	**0.21**	**0.21**	**0.23**	**0.70**	**0.73**	**-0.19**	**0.51**
	12 months	0.25	0.26	0.25	0.29	0.50	0.92	-0.23	0.73

4. CONCLUSION

This research investigated ICM model simulations with SSTA over the Pacific Ocean and Niño 3.4 area. The prediction period was estimated for January to December from 2011 to 2020. The case analysis is separate in two cases:

Case I: Simulation six months in advance (January–June)

Case II: Simulation 12 months in advance (January–December)

In Case I, the time series results from the ICM model showed good trend results in 2011–2016. But, in 2017 and 2018, the time series were underestimated SSTA than ERSST observation. In 2019 and 2020, the ICM model shows a good trend result than in 2017 and 2018, as in the Pacific Ocean case, while, in Niño 3.4 case, the results from the ICM model show a good trend result in 2014–2016 and 2019–2020 period. Since, in 2012 and 2013, the results from ICM show overestimated SSTA but underestimated SSTA in 2017 and 2018.

In Case II, the Pacific Ocean case, the time series from the ICM model showed good trend results in 2013–2015. On the other hand, in 2016–2019, the results were underestimated SSTA than ERSST observation. In mid-2011 and 2013, the ICM model shows an overestimated trend result than ERSST observation. In contrast, the time series from the ICM model shows good trend results in the 2013–2016 and 2019–2020 periods. Since, in 2012, 2013, and 2020 the results from ICM show overestimated SSTA but underestimated SSTA in mid-2015, 2017, and 2018.

From time series analysis, the result from ICM model can capture the highest value in 2016 similar to ERSST observation. The results of the ICM model can indicate a trend of SSTA time series within some period. However, in the time series pattern, the results from Case I (simulation six

months in advance) show a good trend than Case II (simulation 12 months in advance).

In statistical analysis, the statistical value (*R, RMSE, ME*, and *MAE*) of six months in advance were given a good accuracy value from the statistical value from 12 months in advance, as shown in the same direction with the time series pattern in this research. In conclusion, the ICM model was high-performance results to simulate SSTA six months in advance over the Pacific Ocean and Niño 3.4 area.

5. ACKNOWLEDGMENTS

This research was fully supported by the Thai Research Fund (TRF) [RDG6230004] and ARDA [PRP6405031190]. The authors would also like to thank Prof.Dr. Zhu Jiang and Prof.Dr. Zheng Fei from the Institute of Atmospheric Physics (IAP) Chinese Academy of Science for supporting the Intermediate Coupled model (ICM) in this research.

6. REFERENCES

[1] Humphries U., Kaewmesri P., Varnakovid P., and Wongwises P., Improvement in Rainfall Estimates using BiasCorrection with the IAP-DCP Global Model. Mathematics and Computers in Simulation, Vol 171, 2020, pp. 26-35.

[2] Kaewmesri P., and Humphries U., Improving Rainfall Performance by Decaying Average Bias Correction via Lyapunov Theory. International Journal of GEOMATE, Vol 19, Issue 73, 2020, pp.49-56.

[3] Kaewmesri P., Humphries U., Wongwises P., Varnakovida P., Sooktawee Sirapong., and Rajchakit G., Development Simulation of an Unseasonal Heavy Rainfall Event Over Southern Thailand by WRFROMS Coupling Model. International Journal of GEOMATE, Vol 18, Issue 65, 2020, pp.55-63.

[4] Huang B., Thorne P. T., Banzon V. F., Boyer T., Chepurin G., Lawrimore J. H., Menne M. J., Smith T. M., Vose R. S., and Zhang H. M., Extended Reconstructed Sea Surface Temperature, Version 5 (ERSSTv5): Upgrades Validations, and Intercomparisons. Journal of Climate, Vol 30, 2017, pp. 8179-8204

[5] Huang B., Liu C., Ren G., Zhang H. M., and Zhang L., The Role of Buoy and Argo Observation in Two SST Analyses in The Global and Tropical Pacific Oceans. Journal of Climate, Vol 32, 2018, pp. 2517-2535

[6] Huang B., Angel W., Boyer T., Cheng G., Chepurin G., Freeman E., Liu C., and Zhang H. M., Evaluating SST Analyses with Independent Ocean Profile Observations. Journal of Climate, Vol 31, 2018, pp. 5015-5030.

[7] Keenlyside N., Improved Modeling of Zonal Currents and SST in the Tropical Pacific. Ph.D. dissertation, Monash University, 2001, pp. 1-193.

[8] MaCreary J. P., A Linear Stratified Ocean Model of the Equatorial Undercurrent. Philosophical Transactions of Royal Society, Vol 298, 1981, pp.603-635.

[9] Zheng F., Zhu J., Zhang R. H., and Zhou G., Improved ENSO Forecasts by Assimilating Sea Surface Temperature Observations into an Intermediate Coupled Model, Vol 23, Issue 4, 2006, pp. 615-624.

[10] Zheng F., and Zhu J., Coupled Assimilation for An Intermediated Coupled ENSO Prediction Model. Ocean Dynamics, Vol 60, 2010, pp. 1061-1073.

[11] Levitus S., Climatological Atlas of the World Ocean. NOAA Professional Paper, U.S. Government Printing Office, 1982, pp. 1-173.

[12] Kaewmesri P., Humphries U., and Varnakovida P., The Performance of Microphysics Scheme in WRF Model for Simulating Extreme Rainfall Events. International Journal of GEOMATE, Vol 15, Issue 51, 2018, pp.121-131.

[13] Kaewmesri P., Humphries U., and Sooktawee S., Simulation of High-Resolution WRF Model for an Extreme Rainfall Event over the Southern Part of Thailand. International Journal of ADVANCE AND APPLIED SCIENCE, Vol 4, Issue 9, 2017, pp. 26-34.